HOSTED BY

ELSEVIER

Contents lists available at ScienceDirect

Saudi Journal of Biological Sciences

journal homepage: www.sciencedirect.com

الجمعية السعودية لعلوم الحياة
SAUDI BIOLOGICAL SOCIETY

Original article

Medicinal plant extracts interfere in gastric cancer stem cells fluorescence-based assays

Salyoc Tapia-Rojas [a], Marlon García-Paitán [b], Jorge Del Rosario-Chavarri [c], Alexei Santiani [d], Santiago Alvarez-Vega [a], José Amiel-Pérez [a], Ana Mayanga-Herrera [a,*]

[a] Cell Culture and Immunology Lab, Universidad Científica del Sur, Antigua Panamericana Sur km 19, Lima, 15067, Perú
[b] Universidad Nacional Mayor de San Marcos, German Amezaga Av., Lima, 15080, Perú
[c] Plant Biology System Lab, Pontificia Universidad Católica de Chile, Libertador Bernardo O'higgins AV. 340, Santiago, 8331150, Chile
[d] Animal Reproduction Lab, Universidad Nacional Mayor de San Marcos, Circunvalación Av 28, San Borja, Lima, 15021, Perú

ARTICLE INFO

Keywords:
Gastric cancer
Cancer stem cell
Medicinal plants
Interference
Autofluorescence

ABSTRACT

Fluorescence is used in various biological assays due to its high sensitivity, versatility, and precision. In recent years, studies using medicinal plant extracts have increased. However, fluorescence-based assays could be biased by plant metabolites autofluorescence. To address this issue, this study investigated the interference caused by methanolic extracts and chloroform fractions of three medicinal plants in three fluorescence-based assays on gastric cancer stem cells(CSC): resazurin reduction, confocal microscopy, and flow cytometry. CSC were isolated based on CD44 surface marker, incubated with methanolic extracts and chloroform fractions of *Buddleja incana, Dracontium spruceanum, Piper aduncum*. Resazurin assay evidenced that CSC exposed to extracts and fractions from the three plants showed significant differences in relative fluorescence units (RFU) levels ($p < 0.001$) compared to the unexposed groups after a 3-hour incubation. In addition, DMSO-treated CSC exposed to extracts and fractions had significantly lower fluorescence levels than living ones, but higher than extracts and fractions without cells. In confocal microscopy, cancer stem cells exposed to extracts and fractions of *B. incana* and *P. aduncum* were observed in the same emission spectra of the CSC markers. In flow cytometry, CSC exposed to extracts and fractions without any fluorescent dyes were detected in the double positive quadrants for CSC markers (CD44+/CD133 +). Among the three plants, *D. spruceanum* exhibited the least interference. These results show that methanolic extracts and chloroform fractions contain autofluorescent metabolites that interfere with fluorescence-based assays. These results highlight the importance of a prior evaluation for possible fluorescence interference to avoid interpretation biases in fluorescence assays.

1. Introduction

Fluorescence has been used in various biological assays due to its high sensitivity, versatility, speed, accuracy, and reading mode (An, 2009). It has been widely spread within biological research, varying from the evaluation of cell viability with fluorescent dyes, such as DAPI and propidium iodide, to salts that generate a fluorescent compound when reduced by cellular activity, such as resorufin (Lavogina et al., 2022). Fluorescent markers used for the visualization, monitoring, and quantification of individual molecules at cellular level have driven significant advances in understanding cellular processes and dynamics (Specht et al., 2017).

Fluorescent markers that use antibodies bound to fluorochromes are among the most utilized. They enable both quantitative and qualitative analyses of protein expression in various cell types (Mortensen and Larsson, 2001; McKinnon, 2018; Piña et al., 2022). The specificity and sensitivity of these fluorescent markers allow for the determination of the concentration and quantity of target molecules through the analysis of relative fluorescence intensity between control and experimental groups in quantitative approaches (Majumder and Fisk, 2014; Ng et al., 2018; Cheung et al., 2021). In flow cytometry, the specificity of antibodies and broad spectrum of fluorochromes have enabled their

* Corresponding author.
E-mail addresses: stapiar@cientifica.edu.pe (S. Tapia-Rojas), marlon.garcia@unmsm.edu.pe (M. García-Paitán), jldelrosario@uc.cl (J.D. Rosario-Chavarri), asantiania@unmsm.edu.pe (A. Santiani), halvarezv@cientifica.edu.pe (S. Alvarez-Vega), jamielp@cientifica.edu.pe (J. Amiel-Pérez), amayanga@cientifica.edu.pe (A. Mayanga-Herrera).

https://doi.org/10.1016/j.sjbs.2024.104000
Received 15 November 2023; Received in revised form 6 April 2024; Accepted 14 April 2024
Available online 15 April 2024

widespread application to identify different cell populations (McKinnon, 2018). Qualitative approaches, on the other hand, utilize fluorescent markers to gather morphological and spatial information about target molecules at subcellular and supracellular levels (Bhadriraju et al., 2007). Immunofluorescent staining is also helpful in stem cell research for studying processes, such as cell differentiation, through the expression of specific proteins (Collier et al., 2017; Tapia-Rojas et al., 2020), molecules involved in stem cell niche signaling pathways (Kassmer et al., 2020), and cancer development (Cheung et al., 2016).

In recent years, studies evaluating medicinal plant extracts on cancer cells have progressed to give scientific support to the ancestral knowledge of these phytoresources and to identify new bioactive compounds that could be applied for treatment or prevention of disease (Saud et al., 2019). *Buddleja incana, Dracontium spruceanum,* and *Piper aduncum* are medicinal plants traditionally used in Peru for hepatic and respiratory illnesses (Enciso et al., 2020), snake bites (Collantes et al., 2011), and wound healing and anti-inflammatory purposes (Herrera et al., 2019), respectively. These plants are currently being studied to evaluate their anticancer potential (Mayanga-Herrera et al., 2020). However, many of these plant extracts contain autofluorescent molecules that may cause interference with the fluorescent markers used in different assays. The most studied plant autofluorescent molecules are chlorophyll, which is excited by ultraviolet, blue, or green light and strongly emits in the red spectrum, and lignin, which has a broad emission range due to the presence of multiple kinds of fluorophores within its molecular structure (Donaldson, 2020). Likewise, different groups of secondary metabolites with bioactive properties may present autofluorescence, such as flavonoids, stilbenes, terpenes, and terpenoids (García-Plazaola et al., 2015).

Few studies have evaluated the autofluorescent interference of plant extract compounds during fluorescent assays, especially when using cancer stem cells as study models. Therefore, the objective of this study was to evaluate the autofluorescent interference of methanolic extracts and chloroform fractions from three medicinal plants in fluorescence-based assays performed on gastric cancer stem cells.

2. Experimental

2.1. General experimental procedures.

Methanol, chloroform, hexane, dimethyl sulfoxide, DMEM/F-12 medium and resazurin were purchased from Merck (Darmstadt, Germany). All the solvents were ACS grade. Fetal bovine serum and antibiotic/antimycotic 100X were obtained from Biowest (Nuaillé, France). CD44 magnetic microbeads, LS column, FcR blocking reagent, MS columns, CD24 Antibody anti-human FITC, CD44 Antibody anti-human PE and CD133/1 Antibody anti-human APC were bought from Miltenyi Biotec (Bergisch Gladbach, Germany).

2.2. Plant material

In this study, we used three traditional medicinal plants of Peru, that are studied by our research group to evaluate their effect on cancer cell lines. *Buddleja incana* was collected from Yacus at Huanuco department (09°57′18.7″S, 76°31′28.8″W), *Piper aduncum* from La Merced, Chanchamayo (11°02′16.5″S, 75°18′54.0″W) and *Dracontium spruceanum* from Lamas at San Martin department (6°2301.8″S, 76° 30′21.6″W). Plants were collected under the permission of the local authority and each specimen was deposited and taxonomically identified at the natural history museum of Universidad Nacional Mayor de San Marcos (Voucher N°190,191 and 192-USM-2018).

2.3. Extracts and fractions from medicinal plants

Methanolic extracts and chloroform fractions were obtained as described by De Ugaz, O. L. (1994) with some modifications. Leaves of *B. incana* and *P. aduncum* were washed and dried at 40 °C for two days, and bulbs (rhizomes) of *D. spruceanum* for four days, then ground and sieved with a 1 mm mesh, obtaining a fine powder. For methanolic extract preparation, 375 g of plant powders was macerated with 1 L of methanol (Merck, 322415) each for five days, protected from light, and concentrated in a rotary evaporator (IKA RV-10, IKA ® -Werke GmbH & Co. KG, Germany) at 35 °C, 34 rpm, and 200 mbar. Chloroform fractions were prepared with 50 mg of the dry weight of the methanolic extract, dissolved in 100 mL of methanol, and liquid–liquid extractions were made sequentially with 100 mL of hexane (Merck, 1043672511) and 100 mL of chloroform (Merck, 288306). In both cases, the solvents were evaporated by a rotary evaporator at 35 °C, 34 rpm, and 200 mbar. Finally, methanolic extracts and chloroform fractions were weighed and dissolved in dimethyl sulfoxide (DMSO) (Merck, 1029522500) at 32 mg/mL concentration and stored at −80 °C until use.

2.4. Cell culture

The gastric cancer cell line AGS (ECACC 89090402) was cultured in DMEM/F-12 medium (Sigma-Aldrich, D8900) supplemented with 10 % heat-inactivated fetal bovine serum (FBS) (Biowest, S1810) and 1X antibiotic–antimycotic (Biowest, L0010) (from now on denominated as complete DMEM) and incubated at 37 °C and 5 % CO_2. The medium was changed every three days, and when the cells reached a confluence between 75 and 80 %, they were split or used for the assays (Mayanga-Herrera et al., 2020).

2.5. Cancer stem cells isolation

For the isolation of cancer stem cells, the protocol of Najafzadeh et al. (2015) was followed with some modifications. AGS cells were collected and resuspended in 1 mL of complete DMEM medium and counted in a Neubauer chamber. Ten million cells were centrifuged at room temperature, 400 xg for 10 min, the supernatant was discarded, and the pellet was resuspended in 10 µL of anti-CD44 magnetic Microbeads (MiltenyiBiotec, 130–113-335), 10 µL of FcR blocker (Miltenyi Biotec, 130–059-901) and 80 µL of staining buffer (1X saline phosphate buffer (PBS) with 2 % bovine serum albumin (BSA), ethylenediaminetetraacetic acid (EDTA) and 0.09 % azide). Then they were incubated in darkness at 4 °C for 15 min and washed with 1 mL of 1X PBS. The pellet was resuspended in 500 µL of staining buffer and, for magnetic separation, it was transferred to an MS column (Miltenyi Biotec, 130–042-201) attached to the MiniMACS platform (Miltenyi Biotec, 130–090-312), which was previously washed three times with 500 µL of staining buffer. Finally, the cells labeled with the CD44 antibody attached to the column were eluted and cultured at 37 °C and 5 % CO_2. The cells were analyzed by flow cytometry to determine the percentage of CD44 + cells.

2.6. Resazurin cell viability assay

For this assay, the experiment was divided into six groups: 1) complete DMEM without cells, 2) complete DMEM with methanolic extract or chloroform fraction from each plant, 3) complete DMEM with cancer stem cells, 4) complete DMEM with cancer stem cells and methanolic extract or chloroform fraction, 5) complete DMEM with dimethyl sulfoxide (DMSO)-treated cancer stem cells (dCSC) 6) complete DMEM with dCSC and methanolic extract or chloroform fraction. The final concentration of each methanolic extract or chloroform fraction was 160 µg/mL. Each group was replicated three times, except for groups 1 and 2, which were replicated six times.

Gastric cancer stem cells, AGS CD44+, were seeded into a 96-well plate at a concentration of 5 x 10^3 cells/mL for the containing cells groups (3, 4, 5 and 6). Plates were incubated at 37 °C, 5 % CO_2 for 12 h; then, the medium was replaced by 100 µL of the groups indicated above and incubated for 30 min. Then, 20 µL of resazurin (0.15 mg/mL) (Merck, R7017) was added to each well, except in half of replicates of

groups 1 and 2. Fluorescence was measured with an excitation wavelength of 530/20 nm and detected at 590/20 nm on a multimode plate reader (Synergy LX, Biotech) at 3 h after resazurin addition.

2.7. Confocal microscopy assay

The AGS CD44 + cancer stem cells were seeded onto 20x20 mm sterile glass coverslips, previously placed in a 6-well plate, with complete DMEM, incubated at 37 °C, and 5 % CO_2 for 12 h. Next, the culture medium was replaced with methanolic extracts or chloroform fractions dissolved in complete DMEM from each plant in six different coverslips. Other coverslips were used as control and were not exposed to the extract or fraction of medicinal plants. All coverslips were incubated for one hour under the same conditions. Afterward, each coverslip was washed with 1X PBS, and 4 % paraformaldehyde (4 % PFA) was added to fix the cells for 15 min. The coverslips were washed thrice with 1X PBS, stained with 1X 4′,6-diamidino-2-phenylindole (DAPI) for 30 min, and washed with 1.5 mL of 1X PBS. For slides without extract or fraction, in addition to DAPI staining, 5 µL of CD24-FITC antibody, 1 µL of CD44-PE, and 1 µL of CD133-APC diluted in 93 µL of staining buffer were added. Another group of coverslips was maintained without exposure to the extract or fraction and without antibodies as a background control. All coverslips were mounted on microscope slides for observation in the confocal microscope (FluoView™ FV10i, OLYMPUS) excited at 405, 473, 559, and 635 nm.

2.8. Flow cytometry

Flow cytometry assays were conducted as recommended by Gupta et al. (2011). Gastric cancer stem cells, AGS CD44+, were detached with 1X accutase and centrifuged at 400 x g. The supernatant was discarded, and the pellet, containing 4 x 10^5 cells, was resuspended in 800 µL staining buffer and distributed in eight 1.5 mL microtubes. In seven of eight microtubes, 1 µL of CD44-PE antibodies (Miltenyi), and 0.5 µL of each methanolic extract or chloroform fractions of medicinal plants were added until reaching a final concentration of 160 µg/mL. The last microtube was left untreated, only with 0.5 % DMSO as control vehicle. All treatments were incubated for 1 h, washed three times with 1 mL of staining buffer, and finally resuspended in 200 µL of staining buffer. Before sample acquisition, fluorescence compensation was made with FITC, PE, and APC fluorochromes. Samples were acquired on the Flow Cytometer Amnis flowsight imaging (Merck), an imaging flow cytometer (Amnis Flowsight) that has five detection channels for the 488 nm laser (Ch02: 505–560 nm, Ch03: 560–595 nm, Ch04: 595–642 nm, Ch05: 642–740 nm and Ch06: 740–800 nm) and two channels for the 642 nm laser (Ch11: 642–740 nm and Ch12: 740–800 nm), equipped with an image analyzer system. The dot plot was configured to detect the markers CD44-PE and CD133-APC in channels 03 and 11, respectively, and CSCs were evaluated without fluorochromes but previously exposed to the extracts and fractions of *Buddleja incana, Dracontium spruceanum*, and *Piper aduncum*, except in the control group, which was not stained with fluorochromes or treated with extracts or fractions.

2.9. Data analysis

Resazurin assay data were analyzed using the statistical program GraphPad Prism V.8.0.0 for Windows. One-way ANOVA was used to compare the results of each experimental group, followed by a Post Hoc analysis of multiple Tukey comparisons, where $p < 0.05$ was considered a significant difference. The values are represented as the mean ± standard deviation (n = 3). Confocal microscope images were analyzed using ImageJ. Flow cytometry data were analyzed using the IDEAS® software version 6.2 (Amnis corporation) for generating dot plots and images.

3. Results

3.1. Resazurin cell viability assay

Our results show that, for the methanolic extracts and fractions evaluated (Fig. 1), there is resazurin reduction in groups 3 (Only CSC) and 4 (CSC with extract or fraction), as evidenced by relative fluorescence units (RFU) values. However, there was minimal resazurin reduction in groups 1 (onlye medium) and 2 (medium with extract or fraction), and 5 (only dCSC) and 6 (dCSC, with extract or fraction). Further, the RFU values in groups 2, 4, and 6 (with methanolic extracts or fractions) were mostly significantly higher than groups 1, 3 and 5 (without any plant extracts or fractions). The RFU values obtained from the cell viability assay with resazurin are summarized in Table S1.

3.2. Cancer stem cells characterization by confocal microscopy

CD24, CD44, and CD133 are commonly used membrane surface markers to identify and characterize gastric cancer stem cells (Tapia, 2022; Lin et al., 2021). In this study, AGS CD44 + cells were confirmed by confocal microscopy, supporting evidence of the presence of cancer stem cells (Fig. 2).

Fluorescence was detected in the cytoplasm of AGS CD44 + cells incubated with chloroform fractions of *B. incana*, *P. aduncum* and *D. spruceanum* as observed in four different channels. However, in the control group, fluorescence was only observed in the channel for detecting DAPI, but no fluorescence was detected in other channels (Fig. 2).

3.3. Flow cytometry analysis of cancer stem cells

The results of imaging flow cytometry showed that when treated with extracts and fractions, CSCs displayed fluorescence in channels 02, 03, 04, 05, 06, and 11. The highest fluorescence intensity was observed in cells treated with methanolic extracts than chloroform fractions. In contrast, the control cells showed no fluorescence at all. These findings are highlighted in Fig. 3.

Fig. 4 displays the percentages of cells stained with extracts and fractions that could have tested positive for CD44-PE and CD133-APC markers, if used. In the control group (unstained CSC), the region where double positives (+/+) are evaluated shows a percentage of 0.7 %, while tCSC treated with methanolic extract of *B. incana* were 100 %, *D. spruceanum* were 14.5 %, and *P. aduncum* were 69.9 %. On the other hand, CSCs that were treated with the chloroform fraction of *B. incana*, *D. spruceanum*, and *P. aduncum* showed as 68.1 %, 2.9 %, and 73.5 %, respectively.

4. Discussion

In this study, we performed three fluorescence-based assays for analyzing cancer stem cells previously exposed to methanolic extracts and chloroform fractions, demonstrating that plant metabolites fluorescence could interfere and lead to biased results.

Resazurin is a non-fluorescent compound that, when reduced, is converted into resorufin, a fluorescent compound, with a maximum excitation at 544 nm and emission within the spectrum of yellow-orange color with a peak at 590 nm (Balbaied and Moore, 2020). This emission range is similar to some secondary metabolites contained in plants (Donaldson, 2020), including polyacetylenes, anthraquinones, anthocyanins, alkaloids, and tannins (García-Plazaola et al., 2015).

Alkaloids and tannins have been reported in *D. spruceanum* (Rivera-Parada, 2013), anthocyanins in *B. incana* (Enciso et al., 2020), and flavonoids and quinones in *P. aduncum* (Mayanga-Herrera et al., 2020; Arroyo et al., 2011). These metabolites have an autofluorescent emission in the yellow-orange spectrum, similar to resorufin, however, in this experiment no significant increase in the fluorescent signal was

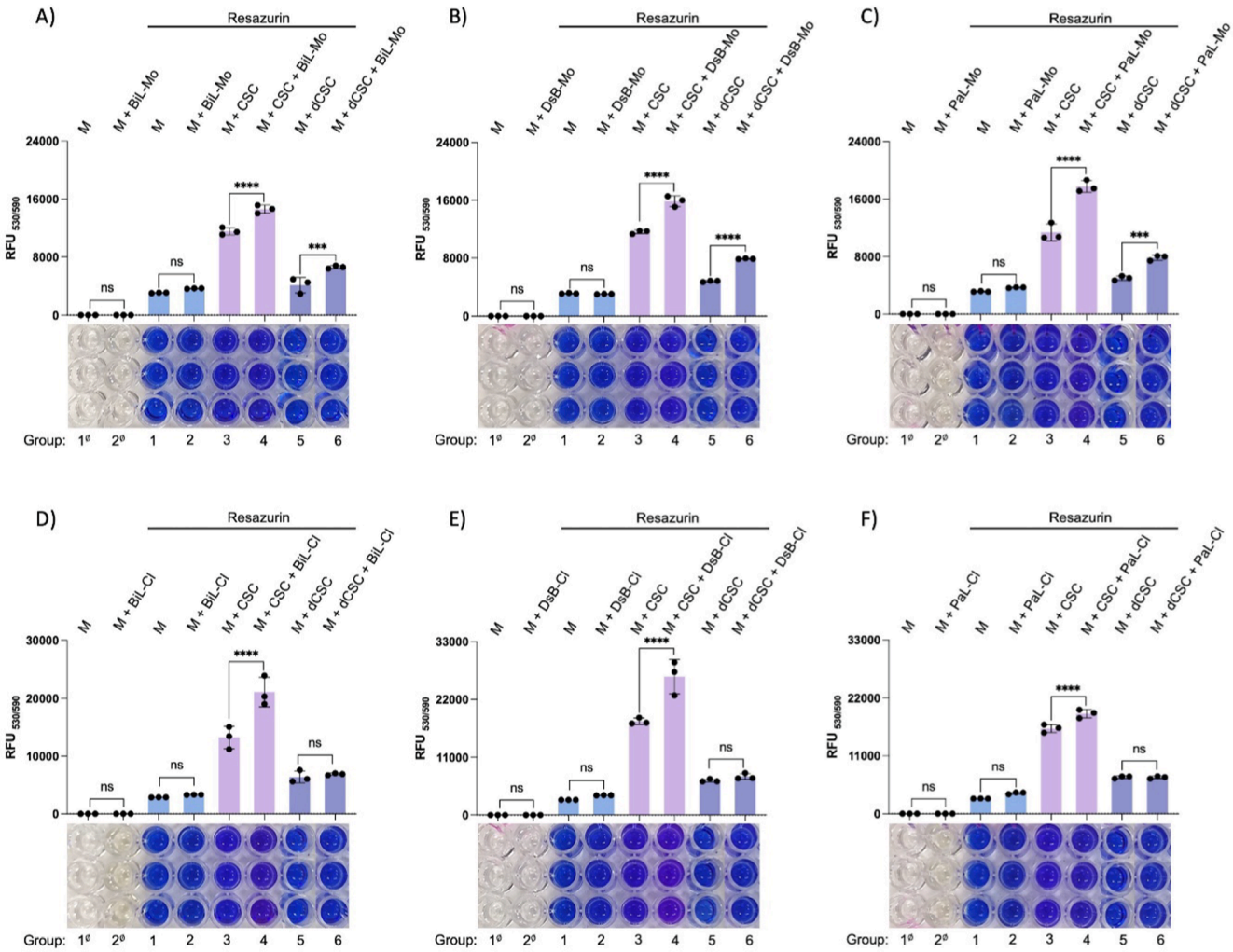

Fig. 1. Fluorescence generated by methanolic extracts (Mo) and chloroform (Cl) fractions of *Buddleja incana* leaves (BiL) (A and D), *Dracontium spruceanum* bulb (DsB) (B and E), and *Piper aduncum* leaves (PaL) (C and F), and its interaction with CSC by resazurin viability assay. M: medium, CSC: Cancer Stem Cells, dCSC: DMSO-treated Cancer Stem Cells, RFU: relative fluorescence units. **Groups: 1**: complete DMEM, **2:** complete DMEM + methanolic extract/chloroform fraction, **3:** complete DMEM + CSC, **4:** complete DMEM + CSC + methanolic extract/chloroform fraction, **5:** complete DMEM + dCSC, **6:** complete DMEM + dCSC + methanolic extract/chloroform fraction. $^{\Phi}$: Groups without resazurin. (****) $p < 0.0001$, (***) $p < 0.001$, **ns:** non-significant.

observed in the groups with methanolic extracts or fraction, but without cells and resazurin (Fig. 1). Although a non-significant higher signal was observed in extract treatments with resazurin compared to medium alone, this phenomenon can be attributed to the antioxidant capacity of some plant extracts, as these are often reducing agents (Yadi et al., 2018), which could cause the reduction of some resazurin molecules to resorufin, resulting in increased fluorescence. This possibility comprises the three plant species analyzed, since they have reported antioxidant activity in their extracts (Ingaroca et al., 2018; Paredes-López et al., 2018; Enciso et al., 2020).

Our results showed that groups containing living cells, with or without exposure to extracts or fractions, displayed higher levels of RFU compared to other treatments. This is due to the reduction of resazurin to resorufin resulting from cellular metabolism, mainly through mitochondrial enzymes (Präbst et al., 2017). The groups with plant extracts or chloroform fractions showed significantly higher RFU levels than the other groups. This difference is likely caused by the interaction of compounds between CSC molecules and the metabolites of the plant extract or chloroform fraction, e.g. isorhamnetin, quercetin, vitexin, yangonin, fisetin, morin (Zou et al., 2002; Sentchouk and Bondaryu, 2007), which increases autofluorescence. This phenomenon has also been observed in human lymphocytes (Ottoni et al., 2019). The fluorescence of certain metabolites, such as quercetin, has been observed to increase 10-fold when found in a less polar medium (Sentchouk and Bondaryu, 2007), as in this study where the extracts or fractions are dissolved in 0.5 % DMSO. Additionally, there can be an increased substitution of oxygenated species to benzenes of phenolic compounds that cause an increase in the intensity of fluorescence (Williams and Bridges, 1964). The fluorescence increase is mainly due to the extracts antioxidant capacity and cells redox potential (Jiang et al., 2014).

In this study, it was observed that groups with extract or fraction showed a higher level of RFU, usually regarded as cell proliferation. However, it cannot be interpreted as an increase in the number of viable CSCs because the incubation time with the extract or fraction was only 3 h. This period is insufficient to observe cell growth proportional to the RFU values obtained. In addition, images from the inverted microscope did not show differences in the number of cells per well (Figure S1). Therefore, this misinterpretation would generate a type II error, false negative for cytotoxicity tests, and type I error, false positive for cell proliferation tests. On the other hand, groups containing dCSC had higher levels of RFU compared to the groups that only contained cell culture medium. This difference could be attributed to the residual presence of autofluorescent molecules accumulated before cell death,

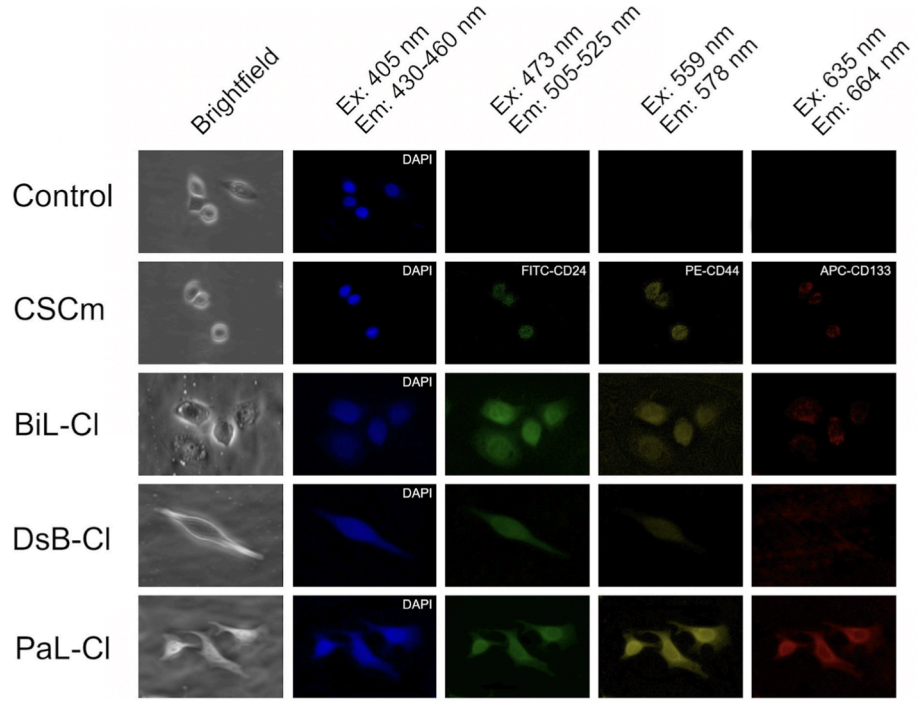

Fig. 2. Confocal microscopy images at 25X magnification of AGS CD44 + gastric cancer stem cells (CSC) stained with stem cells markers or treated with chloroform fractions. Control: CSC not stained nor treated with any fractions. CSCm: CSC stained anti-CD24/FITC, anti-CD44/PE and anti CD133/APC (gastric cancer stem cell markers). Control: Cells not treated with any extract or fractions.

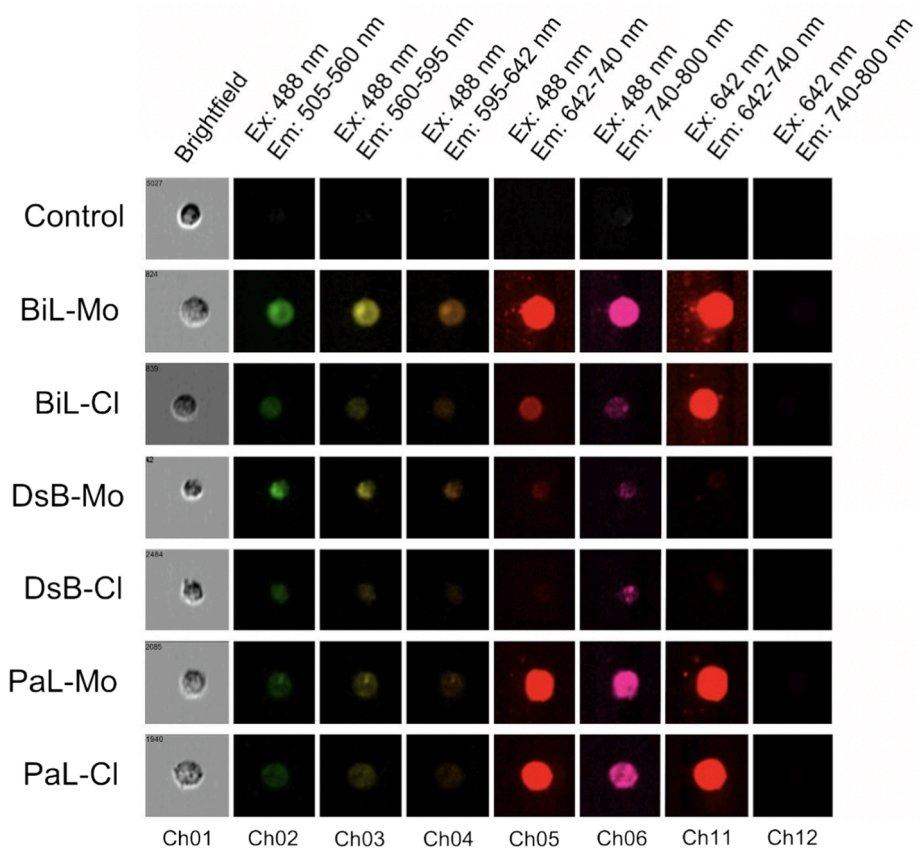

Fig. 3. Representative images of a single AGS CD44 + cancer stem cell (CSC) in imaging flow cytometry treated with methanolic extracts (Mo) or chloroform fractions (Cl) of *Buddleja incana* leaves (BiL), *Dracontium spruceanum* bulb (DsB), and *Piper aduncum leaves* (PaL). Control: CSC not stained nor treated with any extract or fraction. Lasers: 488 and 642 nm.Ch: Channel. Ex: Excitation wavelength. Em: Emission wavelength.

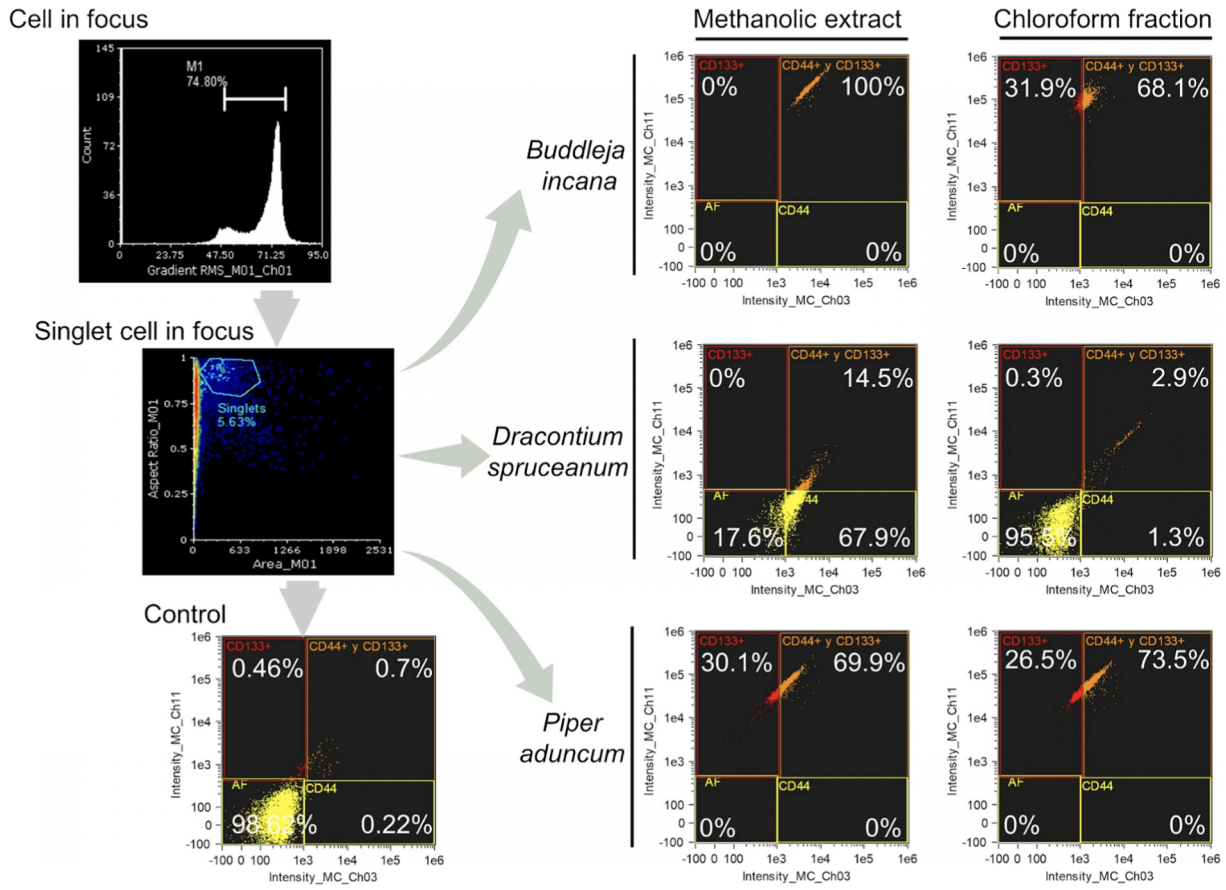

Fig. 4. Flow cytometry dot plots showing four quadrants and schematic gating of AGS cancer stem cells (CSC) treated with methanolic extracts or chloroform fractions of *Buddleja incana*, *Dracontium spruceanum*, and *Piper aduncum*, in channels Ch03 (560–595 nm) and Ch11 (642–740 nm). Control: CSC not stained nor treated with any extract or fraction. Lasers: 488, and 642 nm.

such as flavins, which have a fluorescent emission that covers the yellow-orange spectrum (Shilova et al., 2017) and accumulate under conditions of cellular stress (Surre et al., 2018). Additionally, the residual presence of NAD(P)H, product of mitochondrial dysregulation (Aleshin et al., 2015,) and the enzymatic activity present after cell death (Tan and Qian, 1996), could contribute to the reduction of resazurin to resorufin to raise the fluorescent signal in the treatment with dCSC.

A significant difference in RFU levels was observed between the groups of dCSC treated with methanolic extract and untreated. This difference can be attributed to the sequential process used to obtain the methanolic extract and the chloroform fraction, which have different polarities. The methanol phase, due to its high polarity, extracted a higher number of metabolites, while the chloroform phase, being less polar, extracted a smaller amount of metabolites (Mayanga-Herrera et al., 2020). Methanol is known for its high power to extract various active components because of its polar nature, and it is widely used as a solvent for extraction processes (Cowan, 1999; Madani et al., 2021). However, studies indicate that methanol could lead to the generation of artifacts during the extraction process, which may be detected at the same wavelengths of flavonoids, carotenoids, tetrapyrroles, fatty acids, among others (Sauerschnig et al., 2018). These artifacts might interact with residual molecules from cells and the culture medium, such as bovine serum albumin, potentially causing an increase in fluorescence (Sentchouk and Bondaryu, 2007). On the other hand, chloroform is a solvent with lower polarity, and it extracts fewer metabolites, generating a fraction free of tannins and rich in terpenoids and flavonoids (Chethankumara et al., 2021; Jones and Kinghorn, 2012). A lower level of RFU at 590/35 nm was observed in groups 5 (only dCSC, which were dead) and 6 (dCSC with extraction or fraction) when treated with chloroform fraction in comparison to those treated with methanolic extract, probably due to that most of the compounds were retained in the first extraction with methanol, whereas chloroform, being less polar, extracts a smaller amount of metabolites (Cowan, 1999; Madani et al., 2021).

In confocal microscopy, CSCs treated with *P. aduncum* exhibited the highest fluorescence in the four emission spectra compared to the other plant treatments. The autofluorescence in the green spectrum may be caused by alkaloids and flavonoids (Arroyo et al., 2011), while the yellow emission may be attributed to quinones, tannins, and alkaloids. On the other hand, the red emission is only attributed to quinones (Talamond et al., 2015; Donaldson, 2020). Furthermore, fluorescence was detected in the cytoplasm in the blue emission spectrum that overlaps with DAPI. This cytoplasmic stain is not seen in the control group or dCSC and can be associated with certain phenols and alkaloids present in *P. aduncum*, which can emit in the blue spectrum (Arroyo et al., 2011; Donaldson, 2020). Additionally, the autofluorescence in this group was visible throughout the cell, indicating that its phytochemical compounds could be interacting with molecules of different cellular compartments.

In CSCs treated with the chloroform fraction of *B. incana*, fluorescence was detected in the green and yellow spectra and slight staining of the cytoplasm in the blue and red emission spectrum. Within the phytochemical components reported for *B. incana*, the blue emission can be caused by phenolic compounds, coumarins, and alkaloids; the green emission by flavonoids, terpenoids, tannins, and alkaloids; the yellow emission by alkaloids and tannins (Enciso et al., 2020); and the red emission by leucoanthocyanidins (Talamond et al., 2015; Donaldson, 2020). The autofluorescence intensity was higher in the green emission

spectrum and decreased in the yellow, blue and red spectra covering different cell compartments.

CSCs treated with the chloroform fraction of *D. spruceanum* showed fluorescence in blue and green emission spectra and a weak stain in the yellow emission. The cytoplasm fluorescence in the blue spectrum can be attributed to alkaloids and coumarins present in the plant; the emission in green to flavonoids, tannins, terpenoids, and alkaloids (Rivera-Parada, 2013); and the weak signal in yellow emission to some alkaloids (Talamond et al., 2015; Donaldson, 2020). Unlike the other plants, *D. spruceanum* chloroform fraction caused minor interference to fluorescent markers for CSCs, which would allow any fluorophore to be used in the yellow and/or red spectrum; additionally, fluorescent CSC characterization tests would need only normalization in the green emission spectrum with this fraction. In all treatments, emission in the blue spectrum could also be intensified by the accumulation of NAD(P)H produced by the metabolic stimulus of exposure to chloroform fractions (Croce and Bottiroli, 2014).

Flow cytometry images from CSCs treated with extracts and fractions show in the majority of channels, either in greater or lesser intensity. The methanolic extracts of *B. incana*, *D. spruceanum*, and *P. aduncum* generated greater fluorescence intensity in the CSCs than those treated with chloroform fractions. This could have been due to the methanolic extracts containing a more significant amount and variety of autofluorescent metabolites, unlike the chloroform fractions, attributed to the sequential process done to obtain them (Mayanga-Herrera et al., 2020), the degree of polarity of the solvents (Cowan, 1999), and the high extraction power of methanol (Madani et al., 2021) as opposed to chloroform, as mentioned above.

The methanolic extract of *B. incana* presented the highest fluorescence in all emission spectra, which indicates a greater bioavailability of the metabolites present in the extract that exhibit autofluorescence, such as alkaloids, flavonoids, anthocyanins, and tannins (Donaldson, 2020; Enciso et al., 2020). The bioavailability of metabolites also allows more significant chemical interaction with cellular components that can lead to increased fluorescence (Ottoni et al., 2019). This intense fluorescent signal from treatments with the methanolic extract of *B. incana* and *D. spruceanum* could generate significant interference in the emission and excitation channels of the flow cytometer, which would avoid a correct interpretation when using fluorescent markers. This inconvenience increased in the red (642–740 nm) and far red (740–800 nm) emission spectra, where a strongly cellular fluorescence signal was observed in the methanolic extract of *B. incana* and methanolic extract and fraction of *P. aduncum* apparently due to the fluorescence spectrum of chlorophyll present in the leaves used to obtain the extract of these species (García-Plazaola et al., 2015).The methanolic extract of *B. incana* showed the highest fluorescence in all emission spectra. This indicates a greater bioavailability of the metabolites present in the extract, which exhibit autofluorescence, such as alkaloids, flavonoids, anthocyanins, and tannins (Donaldson, 2020; Enciso et al., 2020). The bioavailability of these metabolites allows for more significant interaction with cellular components, leading to increased fluorescence (Sentchouk and Bondaryu, 2007). However, this intense fluorescent signal from treatments with the methanolic extract of *B. incana* and *D. spruceanum* could cause significant interference in the emission and excitation channels of the flow cytometer, which could result in an incorrect interpretation when using fluorescent markers. This problem increased in the red (642–740 nm) and far red (740–800 nm) emission spectra, where a strong cellular fluorescence signal was observed in the methanolic extract of *B. incana*, as well as in the methanolic extract and fraction of *P. aduncum*. This strong fluorescence signal is apparently due to the fluorescence spectrum of chlorophyll present in the leaves used to obtain the extract of these species (García-Plazaola et al., 2015).

It was observed that CSCs have lower fluorescence intensity than those analyzed in confocal microscopy. This difference can be attributed to the fixation processes performed in confocal microscopy, where aldehyde-derived fixators are known to undergo condensation reactions with amines and proteins, generating fluorescent products (Croce and Bottiroli, 2014).

In fluorescence-based assays, an imaging flow cytometer is advantageous as it enables individual cell visualization, allowing the identification of available detection channels with no interference. It also considers the possibility of compensation to avoid false positive or negative results. In contrast, conventional flow cytometry only relies on the percentage of positive cells for a particular fluorescent marker, which can lead to erroneous interpretations of results when interference occurs in the same detection channel. The interference of extracts and fractions can be detected in these channels, which may interfere with future assays for the analysis of CSC markers.

Imaging flow cytometry showed autofluorescence for all extracts and chloroform fractions due to the chemical nature of the metabolites present. This can mainly be attributed to the alkaloids existent in *D. spruceanum* (Rivera-Parada, 2013), alkaloids and tannins in *B. incana* (Enciso et al., 2020), and quinones, tannins, and alkaloids in *P. aduncum* (Talamond et al., 2015). Furthermore, a solid fluorescent signal was observed in the extracts of *B. incana* and *P. aduncum*, which can be attributed to the quinones and leukocyanidins present respectively in these plant species (Arroyo et al., 2011; Enciso et al., 2020). However, the most significant contribution of fluorescence could be generated by protochlorophyllide, since it is excited and emits fluorescence within the range of the red spectrum (Amirjani and Sundqvist, 2006). Instead, fluorescence was not observed in *D. spruceanu*m extracts due to their non-foliar nature as a raw material for making the extract.

These results detail the importance of evaluating the excitation and emission channels generated by fluorescence because of the plant extract, and then choosing immunofluorescent markers in the channels where no interference is generated or that can be compensated. This is a procedure that might be ignored during investigations (Ottoni et al., 2019). Moreover, the employment of modern equipment such as the spectral cytometer allows for the analysis of the full spectrum of both cellular autofluorescence and the fluorophores used, providing advantages in compensation. Similarly, the mass cytometer, also known as cytometry by Time-Of-Flight (CyTOF), uses antibodies conjugated with heavy metals instead of fluorophores (Jaimes et al., 2022). However, it's important to note that these advanced equipment are not widely available, which would make their use challenging.

5. Conclusions

The methanolic extracts and chloroform fractions of *Buddleja incana*, *Dracontium spruceanum*, and *Piper aduncum* contain autofluorescent metabolites that interfere with fluorescence-based assays performed on cancer stem cells. The autofluorescence of methanolic extracts and chloroform fractions, not being in contact with cancer stem cells, does not generate significant fluorescence levels. Nonetheless, in presence of resazurin, metabolites present in extracts or fractions can reduce it to resorufin, causing fluorescence levels (RFU) to increase. Cancer stem cells contain autofluorescent compounds from cell activity, which have conjugated rings as chemical structures, such as NAD(P)H, FAD, and flavins, among others that can interact with some plant metabolites, such as flavonoids, tannins, alkaloids, and others, which significantly contribute to fluorescence increase. Methanolic extracts and chloroform fractions mask the detection of gastric cancer stem cell surface markers, CD24, CD44, and CD133, in confocal microscopy assays. Similarly, these extracts and fractions interfere with flow cytometry assays, both qualitative and quantitative analysis.

These results highlight the importance of a prior evaluation of the fluorescence generated when using methanolic extracts and chloroform fractions in fluorescence-based assays on cancer stem cells to avoid interpretation biases and look for channels where there is no interference or where interference can be normalized or compensated according to the type of test desired to run.

CRediT authorship contribution statement

Salyoc Tapia-Rojas: Conceptualization, Data curation, Formal analysis, Investigation, Methodology, Writing – original draft, Writing – review & editing, Supervision, Validation, Visualization. **Marlon García-Paitán:** Data curation, Writing – original draft, Writing – review & editing. **Jorge Del Rosario-Chavarri:** Investigation, Resources, Writing – original draft. **Alexei Santiani:** Data curation, Resources, Writing – original draft. **Santiago Alvarez-Vega:** Investigation, Writing – original draft, Writing – review & editing. **José Amiel-Pérez:** Funding acquisition, Methodology, Project administration, Supervision, Writing – original draft. **Ana Mayanga-Herrera:** Conceptualization, Data curation, Formal analysis, Funding acquisition, Investigation, Methodology, Project administration, Resources, Supervision, Validation, Visualization, Writing – original draft, Writing – review & editing.

Declaration of competing interest

The authors declare that they have no known competing financial interests or personal relationships that could have appeared to influence the work reported in this paper.

Acknowledgements

We gratefully acknowledge the funding support from the "Semilla docente 2021" grant provided by Universidad Científica del Sur for this work. We also extend our sincere thanks to Professor Alejando Fukusaki and Dr. Alvaro Marcelo and the Research, Development and Innovation department at Universidad Científica del Sur for providing the necessary laboratory facilities to conduct all the experiments. In addition, we would like to express our appreciation to the Animal Reproduction Laboratory at Universidad Nacional Mayor de San Marcos for allowing us to use the Imaging Flow Cytometer, Amnis FlowSight and to the Molecular biology Lab at Universidad Nacional de Tumbes for the use of the confocal microscope.

Funding

This work was funded by "Semilla Docente 2021" grant given by Universidad Cientifica del Sur, Lima, Perú.

Appendix A. Supplementary data

Supplementary data to this article can be found online at https://doi.org/10.1016/j.sjbs.2024.104000.

References

Aleshin, V.A., Artiukhov, A.V., Oppermann, H., Kazantsev, A.V., Lukashev, N.V., Bunik, V.I., 2015. Mitochondrial impairment may increase cellular NAD(P)H: Resazurin oxidoreductase activity, perturbing the NAD(P)H-based viability assays. Cells 4, 427–451. https://doi.org/10.3390/cells4030427.

Amirjani, M.R., Sundqvist, C., 2006. Red region excitation spectra of protochlorophyllide in dark-grown leaves from plant species with different proportions of its spectral forms. Photosynthetica 44, 83–92. https://doi.org/10.1007/s11099-005-0162-3.

An, W.F., 2009. Fluorescence-based assays. Methods Mol. Biol. 486, 97–107. https://doi.org/10.1007/978-1-60327-545-3_7.

Arroyo, J., Bonilla, P., Tomás, G., Huamán, J., 2011. Estudio fitoquímico del extracto etanólico y de las fracciones de las hojas de Piper aduncum "matico". Rev. Peru. Quím. Ing. Quim. 14, 62–67. https://revistasinvestigacion.unmsm.edu.pe/index.php/quim/article/view/4599.

Balbaied, T., Moore, E., 2020. Resazurin-based assay for quantifying living cells during alkaline phosphatase (ALP) release. Appl. Sci. (basel) 10, 3840. https://doi.org/10.3390/app10113840.

Bhadriraju, K., Elliott, J.T., Nguyen, M., Plant, A.L., 2007. Quantifying myosin light chain phosphorylation in single adherent cells with automated fluorescence microscopy. BMC Cell Biol. 8, 43. https://doi.org/10.1186/1471-2121-8-43.

Chethankumara, G.P., Nagaraj, K., Krishna, V., 2021. In vitro cytotoxic potential of alkaloid and flavonoid rich fractions of alseodaphne semecarpifolia against MCF-7 cells. Biomedical and Pharmacology Journal 14 (2), 557–565. https://doi.org/10.13005/bpj/2158.

Cheung, A.M.Y., Wang, D., Liu, K., Hope, T., Murray, M., Ginty, F., Nofech-Mozes, S., Martel, A.L., Yaffe, M.J., 2021. Quantitative single-cell analysis of immunofluorescence protein multiplex images illustrates biomarker spatial heterogeneity within breast cancer subtypes. Breast Cancer Res. 23, 114. https://doi.org/10.1186/s13058-021-01475-y.

Collantes Díaz, I.E., Gonçalves, G., Yoshida, E., 2011. Chemical constituents from tubers of Dracontium spruceanum (Schott) G. Zhu ex Dracontium loretense Krause (Araceae). Revista De La Sociedad Química Del Perú. 77, 117–126.

Collier, A.J., Panula, S.P., Schell, J.P., Chovanec, P., Plaza Reyes, A., Petropoulos, S., Corcoran, A.E., Walker, R., Douagi, I., Lanner, F., Rugg-Gunn, P.J., 2017. Comprehensive cell surface protein profiling identifies specific markers of human naive and primed pluripotent states. Cell Stem Cell 20, 874–890.e7. https://doi.org/10.1016/j.stem.2017.02.014.

Cowan, M.M., 1999. Plant products as antimicrobial agents. Clin. Microbiol. Rev. 12, 564–582. https://doi.org/10.1128/CMR.12.4.564.

Croce, A.C., Bottiroli, G., 2014. Autofluorescence spectroscopy and imaging: a tool for biomedical research and diagnosis. Eur. J. Histochem. 58, 2461. https://doi.org/10.4081/ejh.2014.2461.

De Ugaz, O.L., 1994. *Investigación Fitoquímica, Métodos en el estudio de productos naturales*, Segunda Edicion. Pontificia Universidad Católica del Perú.

Donaldson, L., 2020. Autofluorescence in plants. Molecules 25, 2393. https://doi.org/10.3390/moleculetable 5102393.

Enciso, J., Pérez, J.A., Miranda, V., Mayanga, A., Tapia, S., Dominguez, F.F., 2020. Uso etnomedicinal, fitoquímica y actividad biológica de la planta andina Buddleja incana Ruiz & Pav. (Scrophulariaceae). Ethnobot. res. appl. 20 https://doi.org/10.32859/era.20.5.1-14.

García-Plazaola, J.I., Fernández-Marín, B., Duke, S.O., Hernández, A., López-Arbeloa, F., Becerril, J.M., 2015. Autofluorescence: Biological functions and technical applications. Plant Sci. 236, 136–145. https://doi.org/10.1016/j.plantsci.2015.03.010.

Gupta, V., Zhang, Q.J., Liu, Y.Y., 2011. Evaluation of anticancer agents using flow cytometry analysis of cancer stem cells. In: Drug Design and Discovery. Humana Press, pp. 179–191. https://doi.org/10.1007/978-1-61779-012-6_11.

Ingaroca, S., Castro, A., Ramos, N., 2018. Composición química y ensayos de actividad antioxidante y del efecto fungistático sobre Candida albicans del aceite esencial de Piper aduncum L. "matico". Rev. Soc. Quím. Perú 85, 268–279. https://doi.org/10.37761/rsqp.v85i2.83.

Jaimes, M.C., Leipold, M., Kraker, G., Amir, E.A., Maecker, H., Lannigan, J., 2022. Full spectrum flow cytometry and mass cytometry: A 32-marker panel comparison. Cytometry Part a. 101, 942–959. https://doi.org/10.1002/cyto.a.24565.

Jiang, J., Auchinvole, C., Fisher, K., Campbell, C.J., 2014. Quantitative measurement of redox potential in hypoxic cells using SERS nanosensors. Nanoscale 6, 12104–12110. https://doi.org/10.1039/c4nr01263a.

Jones, W.P., Kinghorn, A.D., 2012. Extraction of plant secondary metabolites. Methods Mol. Biol. 864, 341–366. https://doi.org/10.1007/978-1-61779-624-1_13.

Kassmer, S.H., Langenbacher, A.D., De Tomaso, A.W., 2020. Integrin-alpha-6+ Candidate stem cells are responsible for whole body regeneration in the invertebrate chordate Botrylloides diegensis. Nat. Commun. 11, 4435. https://doi.org/10.1038/s41467-020-18288-w.

Lavogina, D., Lust, H., Tahk, M.-J., Laasfeld, T., Vellama, H., Nasirova, N., Vardja, M., Eskla, K.-L., Salumets, A., Rinken, A., Jaal, J., 2022. Revisiting the resazurin-based sensing of cellular viability: Widening the application horizon. Biosensors (basel) 12, 196. https://doi.org/10.3390/bios12040196.

Lin, T., Peng, W., Mai, P., Zhang, E., Peng, L., 2021. Human gastric cancer stem cell (GCSC) markers are prognostic factors correlated with immune infiltration of gastric cancer. Frontiers in Molecular Biosciences 305. https://doi.org/10.3389/fmolb.2021.626966.

Madani, A., Mazouni, N., Nedjhioui, M., 2021. Plants' bioactive metabolites and extraction methods. In: Zepka, L.Q., do Nascimento, T.C., Jacob-Lopes, E. (Eds.), Bioactive Compounds. IntechOpen, Londres, Inglaterra., 10.5772/INTECHOPEN.96698.

Majumder, S., Fisk, H.A., 2014. Quantitative immunofluorescence assay to measure the variation in protein levels at centrosomes. J. vis. Exp. https://doi.org/10.3791/52030.

Mayanga-Herrera, A., Tapia-Rojas, S., Fukusaki-Yoshizawa, A., Marcelo-Rodríguez, Á., Amiel-Pérez, J., 2020. Cytotoxic activity of the chloroform fraction of Piper aduncum and its effect on the cell cycle in gastric cancer cell lines. Rev. Peru. Med. Exp. Salud Publica 37, 471–477. https://doi.org/10.17843/RPMESP.2020.373.5157.

McKinnon, K.M., 2018. Flow cytometry: An overview. Curr. Protoc. Immunol. 120, 5.1.1. https://doi.org/10.1002/CPIM.40.

Mortensen, K., Larsson, L.I., 2001. Quantitative and qualitative immunofluorescence studies of neoplastic cells transfected with a construct encoding p53-EGFP. J. Histochem. Cytochem. 49, 1363–1367. https://doi.org/10.1177/002215540104901104.

Najafzadeh, N., Mazani, M., Abbasi, A., Farassati, F., Amani, M., 2015. Low-dose all-trans retinoic acid enhances cytotoxicity of cisplatin and 5-fluorouracil on CD44+ cancer stem cells. Biomedicine & Pharmacotherapy 74, 243–251. https://doi.org/10.1016/j.biopha.2015.08.019.

Ng, S.B., Fan, S., Choo, S.-N., Hoppe, M., Mai Phuong, H., De Mel, S., Jeyasekharan, A.D., 2018. Quantitative analysis of a multiplexed immunofluorescence panel in T-cell lymphoma. SLAS Technol. 23, 252–258. https://doi.org/10.1177/2472630317747197.

Ottoni, M.H.F., Santos, M.G.D., Almeida, V.G.de., Costa, L.de.A., Meireles, A.B., Avelar-Freitas, B.A.de., Santos, J.A.T.D., Pereira, W.de.F., Brito-Melo, G.E.A., 2019. Background autofluorescence induced by plant extracts in human lymphocytes: A

flow cytometric analysis of a critical bias. J. Immunol. Methods 468, 1–9. https://doi.org/10.1016/j.jim.2019.02.007.

Paredes-López, D., Robles-Huaynate, R., Mendoza-Isla, D., Mendoza-Pérez, C., Saavedra-Rodríguez, H., 2018. The effect of the ethanol extract from the Dracontium spruceanum rhizome on hematologic and biochemical profiles and performance parameters of broiler chickens. Sci. Agropecu. 9, 411–416. https://doi.org/10.17268/sci.agropecu.2018.03.12.

Piña, R., Santos-Díaz, A.I., Orta-Salazar, E., Aguilar-Vazquez, A.R., Mantellero, C.A., Acosta-Galeana, I., Estrada-Mondragon, A., Prior-Gonzalez, M., Martinez-Cruz, J.I., Rosas-Arellano, A., 2022. Ten approaches that improve immunostaining: A review of the latest advances for the optimization of immunofluorescence. Int. J. Mol. Sci. 23, 1426. https://doi.org/10.3390/ijms23031426.

Präbst, K., Engelhardt, H., Ringgeler, S., Hübner, H., 2017. Basic colorimetric proliferation assays: MTT, WST, and resazurin. Methods Mol. Biol. 1601, 1–17. https://doi.org/10.1007/978-1-4939-6960-9_1.

Rivera-Parada, L.L., 2013. Caracterización fitoquímica, farmacéutica y alimenticia de Papa culebrera india (Dracontium spruceanum (Schott) GH Zhu, Araceae) y Sande (Brosimum utile (Kunth) Oken, Moraceae) del Jardín Botánico de Plantas Medicinales del CEA de CORPOAMAZONIA, Mocoa, Putumayo. Corporación Para El Desarrollo Sostenible Del Sur De La Amazonia CORPOAMAZONIA 1–11.

Saud, B., Malla, R., Shrestha, K., 2019. A review on the effect of plant extract on mesenchymal stem cell proliferation and differentiation. Stem Cells Int. 2019, 7513404. https://doi.org/10.1155/2019/7513404.

Sauerschnig, C., Doppler, M., Bueschl, C., Schuhmacher, R., 2017. Methanol generates numerous artifacts during sample extraction and storage of extracts in metabolomics research. Metabolites. 8, 1. https://doi.org/10.3390/metabo8010001.

Sentchouk, V.V., Bondaryuk, E.V., 2007. Fluorescent analysis of interaction of flavonols with hemoglobin and bovine serum albumin. Journal of Applied Spectroscopy. 74, 731–737. https://doi.org/10.1007/s10812-007-0117-5.

Shilova, O.N., Shilov, E.S., Deyev, S.M., 2017. The effect of trypan blue treatment on autofluorescence of fixed cells. Cytometry A 91, 917–925. https://doi.org/10.1002/cyto.a.23199.

Specht, E.A., Braselmann, E., Palmer, A.E., 2017. A critical and comparative review of fluorescent tools for live-cell imaging. Annu. Rev. Physiol. 79, 93–117. https://doi.org/10.1146/annurev-physiol-022516-034055.

Surre, J., Saint-Ruf, C., Collin, V., Orenga, S., Ramjeet, M., Matic, I., 2018. Strong increase in the autofluorescence of cells signals struggle for survival. Sci. Rep. 8, 12088. https://doi.org/10.1038/s41598-018-30623-2.

Talamond, P., Verdeil, J.-L., Conéjéro, G., 2015. Secondary metabolite localization by autofluorescence in living plant cells. Molecules 20, 5024–5037. https://doi.org/10.3390/molecules20035024.

Tan, T.C., Qian, Z.R., 1996. Activity of the enzyme system in thermally killed Bacillus cells. Enzyme Microb. Technol. 19, 150–156. https://doi.org/10.1016/0141-0229(95)00235-9.

Tapia-Rojas, S., Mayanga-Herrera, A., Enciso-Gutiérrez, J., Centurion, P., Amiel-Pérez, J., 2020. Procedure for culture and identification of stem cells from human lipoaspirate for research purposes. Revista Peruana De Medicina Experimental y Salud Pública. 37, 547–553. https://doi.org/10.17843/rpmesp.2020.373.5201.

Williams, R.T., Bridges, J.W., 1964. Fluorescence of solutions: A review. J. Clin. Pathol. 17, 371–394. https://doi.org/10.1136/jcp.17.4.371.

Yadi, M., Mostafavi, E., Saleh, B., Davaran, S., Aliyeva, I., Khalilov, R., Nikzamir, M., Nikzamir, N., Akbarzadeh, A., Panahi, Y., Milani, M., 2018. Current developments in green synthesis of metallic nanoparticles using plant extracts: a review. Artif. Cells Nanomed. Biotechnol. 46, S336–S343. https://doi.org/10.1080/21691401.2018.1492931.

Zou, L., Harkey, M.R., Henderson, G.L., 2002. Effects of intrinsic fluorescence and quenching on fluorescence-based screening of natural products. Phytomedicine. 9, 263–267. https://doi.org/10.1078/0944-7113-00121.